ROUND-TRIP TRAJECTORIES FOR MARS OBSERVATION

*Paul G. Johnson and Roger L. Smith**

The characteristics of Earth-Mars round-trip ballistic trajectories are compared in terms of (1) total velocity increment, (2) total trip time, (3) choice of launch date and waiting time, (4) communication distance, and (5) sensitivity to departure-velocity-vector error. Particular emphasis is given short-waiting-time paths. Two families are shown to be of primary interest: (a) low-waiting-time orbiting paths, and (b) perihelion swing-around paths. The analysis is based on the assumption of circular, coplanar planetary orbits.

INTRODUCTION

Not many years hence the science of space flight will have matured to the point where vehicles are capable of making interplanetary round trips and man is ready to go along. In the meantime, research and development in the various technologies which make such an achievement possible should be aimed toward common goals. In particular, development of the more exotic propulsion systems should be directed toward establishment of the capability to perform difficult missions, such as the transport of large payloads on high-energy trajectories. To furnish initial direction to such a diverse effort, a knowledge of the characteristics of interplanetary round trips seems to be urgently needed.

The purpose of this paper is to present an over-all picture of the choices and compromises available in the various families of round-trip ballistic trajectories. To this end the characteristics of several trajectory types have been calculated or compiled from previous studies reported in the literature. The trajectories are then compared in terms of pertinent criteria. Mars has been selected as the destination planet for purposes of illustration, there being as much current interest in observation of Mars as any other planet. Several simplifying assumptions have been made to enhance the presentation, principally those of circular, coplanar planetary orbits. All trips are assumed to start and end in circular satellite orbits about Earth.

The two principal types of round-trip trajectories discussed are (1) paths which go into a closed orbit about Mars, called "orbiting" paths, and (2) paths which have no propulsion requirement at Mars, being deflected onto a return path by the gravitational field of Mars, called "swing-around" paths. The orbiting paths are essentially the same as those proposed by Ehricke [1] and the swing-around paths are the same as Battin [2] called "nonstop" round-trip trajectories.

The selection of a trajectory for a particular round-trip mission will be influenced by many factors. In addition to those characteristics peculiar to the calendar date on which the flight is begun, consideration should be given to attainment of the following:

*Lewis Research Center, National Aeronautics and Space Administration, Cleveland, Ohio.

1. Low total impulse.
2. Short total trip time.
3. Some choice of launch date and waiting time.
4. Short communication distance during Mars observation.
5. Insensitivity to departure-velocity-vector error (low miss coefficients).

Since these factors are not independent, a judicious compromise will be required, taking into account the purposes and economics of the specific mission to be performed.

Assumptions

The subject of interplanetary round trips is rather complex due to the number of parameters which may be varied and the levels of accuracy at which computations may be made. For example, there are times in each synodic period during which Earth-Mars flight is impractical. August 1959 is an example of this, Mars being located roughly 140° behind the Earth. A trajectory to reach Mars beginning at this time would have to be either of unreasonably high energy or of about two-years' duration one way. Rather than choose the latter course it would be preferable to delay launch one year and make a six-month flight using the same energy.

In addition to the effect of planetary relative angular position, there is also a complication due to the inclination of the planets' orbital planes. To correct for the three-dimensional aspect of the flight, the vehicle will have to either (1) leave Earth in a new plane, which contains the Earth's heliocentric (Sun-centered) radius and the rendezvous point on Mars' orbit, or (2) rely on some form of mid-course correction to get into a plane which will make connections with Mars. In either case there will be penalty involved, even in the most unusual circumstance when the departure and destination points lie along the line of nodes (the intersection of the planetary planes). The three-dimensional-effect penalty associated with a round trip of a particular duration and type will vary with time because the planets will be in different positions relative to the line of nodes at the time of each succeeding launch constellation.

Thus, conditions will change from one synodic period to the next with regard to orbital inclination and from one portion of the synodic period to another with regard to planetary constellation (relative angular position). The eccentricity of the planetary orbits adds a third variation, which varies between synodic periods, further complicating the presentation of trajectory information. In order for this preliminary presentation of round-trip trajectory characteristics to be available at an early date and of appropriate clarity, these calendar-date variations have been omitted. They have not been neglected because they are small, for this is certainly not always the case with orbital inclination effects, but rather because they do not permit generalization. Instead, the required launch constellations for trajectory families of interest are presented along with the other path characteristics. It is assumed that the demand for passage to Mars in the next few decades will be such that the flights can be scheduled near the optimum times. The adjustments for orbital inclination are expected to be independent enough to be added later, further reducing the extent of the launching season. Planetary orbit eccentricity will affect spacecraft utility in that a vehicle of given mass ratio will have somewhat different mission capability from one synodic period to the next. These

effects will be time variations superimposed on the general result presented herein.

The matter of accuracy must be approached in terms of the intended use of the study. If a trajectory is to be calculated in order to supply guidance to an actual flight, the desired accuracy is as great as that to which we know the values of astronomical constants. If, on the other hand, the reason for the computation is to establish a rough estimate of vehicle size, time, and effort need not be wasted on precise procedures. The trajectory calculations reported herein and those of other authors referenced are of an approximate nature, as is indicated by the following list of assumptions:

1. The orbital planes of Earth and Mars are assumed to be circular and coplanar.
2. The Sun, Earth, and Mars are represented by inverse-square central-force fields.
3. The spacecraft is assumed to be under the gravitational influence of only one body at a time. No account is taken of transition from one sphere of influence to another in the vicinity of a planet, and the point at which the spacecraft enters or leaves the heliocentric force field is taken to be identical to the planet's position.
4. All powered flight is assumed to occur in the planetary regions and to have no effect on round-trip characteristics. Thus, any acceleration or deceleration times at Mars are included in the waiting times.
5. The relative energy requirements of round-trip trajectories are assumed to be adequately represented for comparison purposes by means of velocity increments. Mass ratios for low-thrust vehicles (with initial acceleration less than about 0.1 g in Earth orbit) would be in a different quantitative relationship from that indicated by the Δv's, but no difference in trends is expected.

Methods

The basic method of comparison is to plot total trip time versus total velocity increment for the various round-trip trajectory families. The extent to which launch date and waiting time can be varied is illustrated by plots of the various trajectory families, and the possibilities of obtaining low communication distance or low miss coefficients are indicated for the trajectories of greatest interest.

Other types or aspects of round-trip trajectories are of interest, and their exclusion in this comparison should not be construed as an indication of oversight or underestimation of importance. Such subjects as continuous-thrust trajectories, multibody calculations, and three-dimensional effects are worthy of separate studies, the results of which should be applied at a later date to a summary of the situation.

The equations used in the calculations reported herein are the classical equations of two-dimensional celestial mechanics, used in the form developed by Moeckel [3]. Specifically, the following equations define the parameters of the heliocentric elliptic paths in terms of radius and perihelion velocity (Fig. 1). The heliocentric angle, θ, from perihelion to a point of radius r is given by

$$\cos\theta = \frac{V_0^2 - \rho}{\rho(V_0^2 - 1)} \tag{1}$$

where

$$\rho = \frac{r}{r_0} \tag{2}$$

and

$$V_0 = \frac{v_0}{v_{c,0}} \tag{3}$$

The subscript zero refers to conditions at perihelion, and $v_{c,0}$ is the circular velocity at perihelion. The velocity, v, at radius r is given by

$$V^2 = V_0^2 - 2\left(1 - \frac{1}{\rho}\right) \tag{4}$$

where

$$V = \frac{v}{v_{c,0}} \tag{5}$$

The angle, α, between the velocity vector and the circumferential direction at radius r is given by

$$\tan\alpha = \frac{\sqrt{\rho^2(V_0^2 - 2) + 2\rho - V_0^2}}{V_0} \tag{6}$$

for $V_0 > 1$. Likewise, the time, t, to travel from perihelion to radius r is given by

$$t = \frac{r_0}{v_{c,0}}\left\{\frac{1}{(2 - V_0^2)^{3/2}}\left[\sin^{-1}\frac{(2 - V_0^2)\rho - 1}{V_0^2 - 1} + \frac{\pi}{2}\right] - \frac{\sqrt{\rho^2(V_0^2 - 2) + 2\rho - V_0^2}}{2 - V_0^2}\right\} \tag{7}$$

for $1 < V_0^2 < 2$.

The values of astronomical constants and distances used in the calculations, also taken from [3] are summarized in Table I.

Values of hyperbolic velocity, the velocity "at infinity" relative to a planet, are determined from the vehicle's velocity and intersection angle when it enters the sphere of influence of the planet using the equation

$$v_h = \sqrt{(v\cos\alpha - v_p)^2 + v^2\sin^2\alpha} \tag{8}$$

TABLE I.—ASTRONOMICAL CONSTANTS AND DISTANCES
(Reference: Moeckel [3])

Body	Sun	Earth	Mars
Mean distance from Sun, miles		$92.9 \cdot 10^6$	$141.5 \cdot 10^6$
Mean orbital velocity, miles/second		18.5	15.0
Force constant, $\mu = GM$, miles^3/second^2	$3.17 \cdot 10^{10}$	$9.60 \cdot 10^4$	$1.026 \cdot 10^4$
Mean diameter, miles		7918	4140

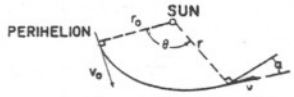

Fig. 1. Illustration of trajectory symbols.

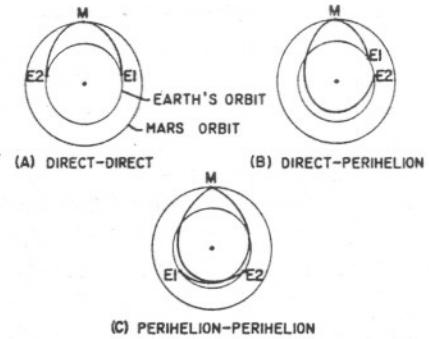

Fig. 2. Schematic of orbiting paths. Only zero-waiting-time trajectories shown.

where v_p is the velocity of the planet in its heliocentric orbit. The velocity increments to enter or leave satellite orbits about the planets are computed by means of the equation

$$\Delta v = \sqrt{v_h^2 + 2\frac{\mu_p}{r_{0,p}}} - \frac{\mu_p}{r_{0,p}} \tag{9}$$

where Δv is the velocity change at the vertex of the hyperbolic approach or departure trajectory (relative to the planet) which would be required to enter or leave a circular orbit at vertex radius ($r_{0,p}$), and μ_p is the force constant of the planet (Table I).

To establish a common base for comparison, orbits about Earth are assumed to be of 300-statute-mile altitude, and orbits about Mars are assumed to be of 1000-statute-mile altitude. In the swing-around maneuver approach altitudes of 300, 1000, and 10,000 statute miles are illustrated, but the 1000-mile altitude is used in the comparison with other round-trip trajectories.

ROUND-TRIP TRAJECTORIES

Orbiting Paths

CONCEPT. In the general case, an Earth-Mars round trip will follow portions of heliocentric elliptic orbits which have no geometrical restrictions other than that they must touch the planets' orbits. The spacecraft would (1) accelerate from a satellite about the Earth and attain a desired hyperbolic velocity, (2) leave the vicinity of the Earth with a velocity which is not necessarily parallel to the Earth's orbit, (3) arrive at Mars with a velocity which is not parallel to Mars' orbit, (4) enter a satellite orbit about Mars by the application of reverse thrust, (5) wait in orbit for some desired time, (6) accelerate onto a homeward path which is not necessarily tangent to the orbits of either Mars or Earth, and (7) enter a satellite orbit about Earth. Since there is always some choice of outbound and return paths available, the characteristics of these trajectories must be examined to determine which ones offer the most desirable combinations of advantages.

Of the various combinations of round-trip trajectories which require the spacecraft to go into a closed orbit about Mars, the three families considered are shown in Fig. 2. Adopting the nomenclature of Vertregt [4], round trips may be

described in terms of the types of paths of which they are composed. The three are: (1) direct-direct, (2) direct-perihelion, and (3) perihelion-perihelion. In Ehricke's chart of mission profiles [1], the equivalent mission profiles are, respectively, 7, 6, and 4 with the removal of any restrictions of tangency with planetary orbits or equivalence between departure and return ellipses. The Hohmann, or minimum-energy, transfer ellipse is the special case which unites the three families, being tangent to the orbits of both Earth and Mars.

Certain special cases of these three trajectory families have been analyzed by Moeckel [3], results of which will be included in the comparison section which follows. Specifically, Moeckel has chosen paths which are tangent at one end or the other. Symmetrical direct-direct and perihelion-perihelion paths are included as well as direct-perihelion paths. The direct-direct paths are shown to involve very long waiting times at Mars, of the order of 500 to 700 days, except at very high values of total velocity increment. For this reason, no computations were made of the general (nontangent) direct-direct round-trip trajectory family, and the data from [3] are used in the comparison as representative characteristics.

Also, within the multitude of orbiting trajectories, selected families can be identified which maximize individual advantages. Two examples are illustrated in this report: (1) "least-energy" paths, which require minimum Δv_{T0t} for specified values of total trip time, and (2) "opposition" paths, which require that Earth and Mars be at their closest approach when the spacecraft is at Mars.

The direct-perihelion paths are the most interesting of the three families. By combining a direct path, during which the Earth travels through a greater angle than does the spacecraft, with a perihelion path, for which the opposite can be true, a round trip of relatively short duration may be obtained. The procedure adopted to present the characteristics of a trajectory family having so many possible combinations is one of isolating those paths which are optimum with respect to specified criteria. In this case, the criteria of low trip time and low total velocity increment are applied; that is, the trajectory families are plotted in terms of t_{T0t} vs Δv_{T0t} and the optimum paths are said to be those farthest to the lowest left. Other criteria, such as low communication distance during waiting time and insensitivity to "burn-out" velocity error, are then applied to the best paths from the $t_{T0t} - \Delta v_{T0t}$ analysis.

The family of perihelion-perihelion trajectories has been given some further study. Moeckel [3] shows, for the condition that the paths be symmetrical and tangent to Mars' orbit, that a waiting time "breakthrough" occurs at a moderate value of total velocity increment. Consequently, slightly asymmetrical paths have been analyzed to determine the optimum paths on a $t_{T0t} - \Delta v_{T0t}$ basis.

Another feature of the perihelion-perihelion trajectory family is that all symmetrical paths are "opposition" paths; that is, the planets are at their closest approach when the spacecraft is at the midpoint of the waiting period. The characteristics of "opposition" paths are presented for use in the over-all comparison.

CHARACTERISTICS. The independent parameters of the orbiting trajectory family are (1) waiting time, (2) velocity magnitude leaving Earth, (3) velocity orientation leaving Earth, and (4) either velocity magnitude or orientation leaving

Mars. Within the ranges over which these parameters may be varied the choice is free, and there results a multitude of possible round-trip paths. To narrow the field, two of these variables have been eliminated on the basis of total time and velocity increment.

For convenience in the computation process the last three parameters were changed to: (2) V_0^2 of the departure path ($V_{0,d}^2$), (3) r_0 of the departure path ($r_{0,d}$), and (4) V_0^2 of the return path ($V_{0,r}^2$). These parameters also define the path. For each specified value of waiting time and $r_{0,d}$, round trips were calculated over a wide range of $V_{0,d}^2$ and $V_{0,r}^2$ combinations. The work charts and computation procedure are presented in the appendix. Plotting total trip time vs total velocity increment, a series of curves for direct-perihelion paths such as Fig. 3a are obtained. Each constant-$V_{0,d}^2$ curve represents a variation of $V_{0,r}^2$ from the lower limit to a value of 1.9. The envelope of these curves is the locus of optimum-$V_{0,r}^2$ points over the specified range of $V_{0,d}^2$. After the envelope curves have been established for several values of $r_{0,d}$, a plot like Fig. 3b can be made. Each constant-$r_{0,d}$ curve represents a variation of $V_{0,d}^2$. The envelope of these curves is the locus of optimum-$r_{0,d}$ points. In this way $r_{0,d}$ and $V_{0,r}^2$ can be optimized on a $t_{T0t} - \Delta v_{T0t}$ basis for any specified value of waiting time. This has been done for direct-perihelion paths with waiting times of 0, 30, and 60 days, and the result is shown in Fig. 3c.

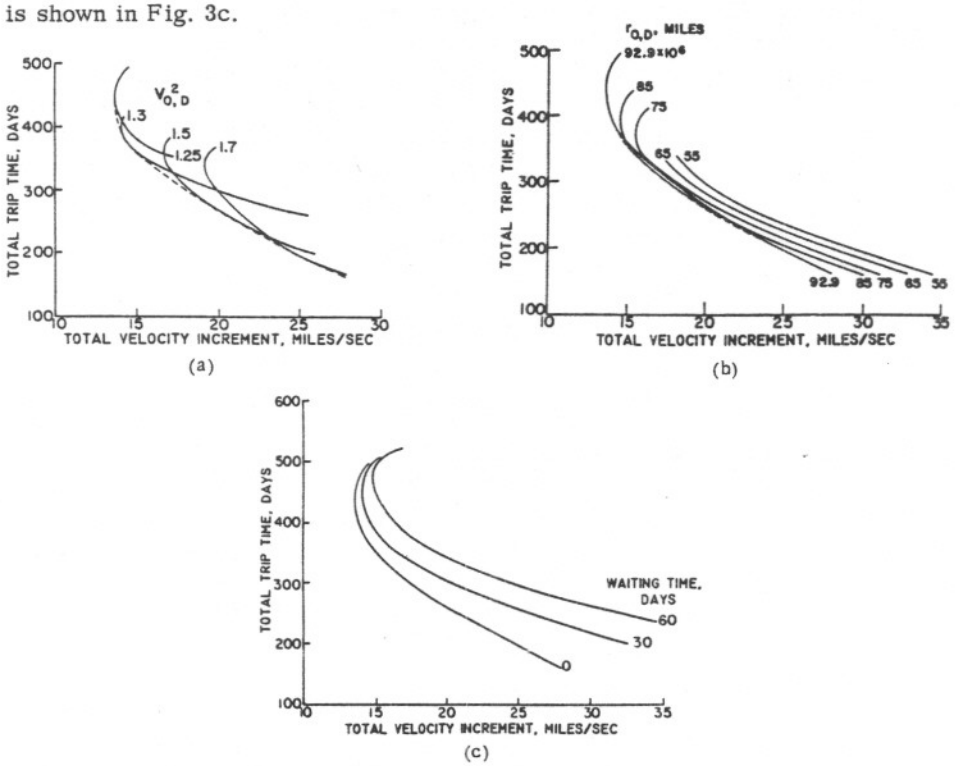

Fig. 3. Characteristics of direct-perihelion orbiting round-trip trajectories. a) Total trip time vs total velocity increment. Departure perihelion radius, $r_{0,d}$, $92.9 \cdot 10^6$ miles; waiting time, t_{wait}, 0 days. b) Total trip time vs total velocity increment. Optimum return path; waiting time, t_{wait}, 0 days. c) Total trip time vs total velocity increment. Optimum return path and departure perihelion radius.

The result of the graphical optimization of direct-perihelion orbiting paths illustrated in Figs. 3a, b, and c is a knowledge of the minimum total velocity increment for any trip time within the range from about 200 to about 500 days for waiting times from 0 to 60 days. The high-$t_{T_{0t}}$ end points correspond to outbound paths tangent at both Earth and Mars. The low-$t_{T_{0t}}$ end points are not physical limits. Rather, the calculations were cut off at a $\Delta v_{T_{0t}}$ of about 30 miles per second.

Figure 3b reveals that the best outbound path is not always tangent to Earth's orbit. For zero waiting time a tangent departure path is optimum at high trip times, but slightly nontangent paths require least energy at lower total trip times. However, the maximum penalty for universal use of tangential departure is only 2.5 percent in $\Delta v_{T_{0t}}$. For the higher waiting times the maximum penalty increases but only to about 6 percent. The optimum flight-path angle relative to Earth's orbit has a maximum value near 12°, occurring at about 300 days coasting flight time for all values of waiting time.

The variation of optimum trip time with waiting time, shown in Fig. 3c, indicates that the coasting time increases with waiting time. This characteristic is illustrated by the fact that total trip time at any specified total velocity increment increases more than 30 days between waiting time curves. The extreme upper ends of the curves are based on extrapolated values, as indicated in the appendix, but the trends are believed to be accurate.

Because the optimum-path characteristics have been obtained graphically, the exact trajectories which make up the envelope curves are not specified. However, it is possible to show the approximate characteristics of the optimum paths. The round-trip trajectories which constitute the optimum-$V_{0,r}^2$ envelope curves from Fig. 3b have been estimated. Only perihelion radii of $92.9 \cdot 10^6$ and $85 \cdot 10^6$ miles have been shown because the optimum radius lies in this range for zero waiting time. The hyperbolic velocities for these paths are shown in Fig. 3d. The return trajectories corresponding to very-low-energy outbound legs are shown to have high hyperbolic velocities, accounting for the hook in the optimum curves at high $t_{T_{0t}}$.

The initial angular position of the planets, shown in Fig. 3e, indicates the choice of launching date for zero-waiting-time direct-perihelion paths. $\Delta\theta_1$ is nearly independent of total trip time for a specified perihelion radius of the departure path. The optimum-$r_{0,d}$ curve is not defined in sufficient detail to draw on this plot, but, since it is along the $92.9 \cdot 10^6$ curve at the high extreme of $t_{T_{0t}}$ and about on the $85 \cdot 10^6$ curve near 300-days trip time, $\Delta\theta_1$ will vary over a range of about 20°. Since Mars and Earth change relative angular position at about 0.5° per day, 20° on the $\Delta\theta_1$ scale corresponds to about 40 days. There will be very little reduction in mission capability in this time period.

The variation of planetary relative angular position at the time when the spacecraft is in orbit about Mars ($\Delta\theta_W$) is shown in Fig. 3f plotted as a function of total trip time and perihelion radius of the departure path for zero-waiting-time paths. Noting that a $\Delta\theta_W$ of 43.1° corresponds to a communication distance twice that of closest approach and a $\Delta\theta_W$ of 27.3° corresponds to a distance ratio of 1.5, it can be seen that the communication distance increases with total trip time. However, the maximum value is not prohibitive.

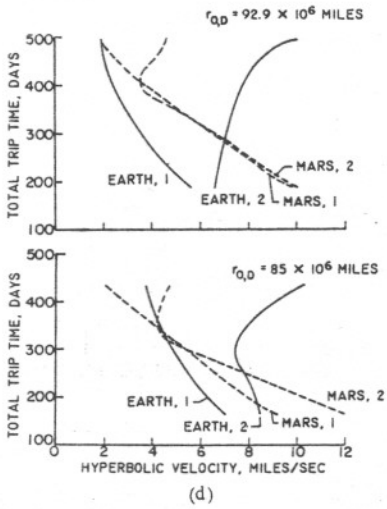

(d)

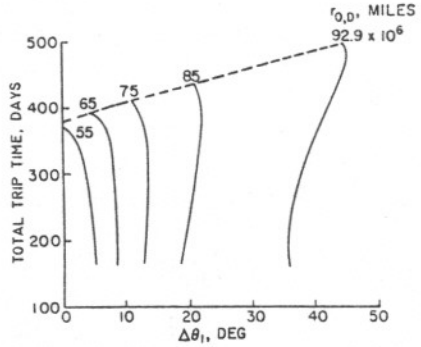

(e)

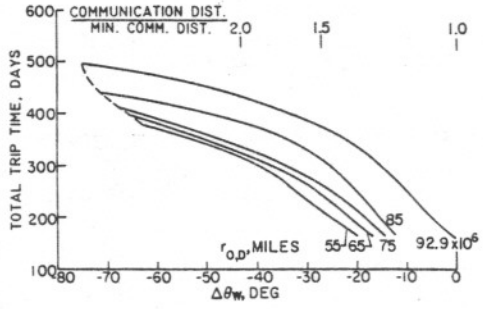

(f)

Fig. 3. Characteristics of direct-perihelion orbiting round-trip trajectories. d) Total trip time vs hyperbolic velocities. Waiting time, t_{wait}, 0 days. e) Total trip time vs planetary relative angular position at Earth departure. Waiting time, t_{wait}, 0 days. Mars is ahead of Earth when $\Delta\theta > 0$. f) Total trip time vs planetary relative angular position when spacecraft is at Mars. Waiting time, t_{wait}, 0 days. Mars is ahead of Earth when $\Delta\theta > 0$.

The characteristics of the perihelion-perihelion orbiting paths, obtained by a process similar to that illustrated for direct-perihelion paths, are shown in Fig. 4. The high-t_{T0t} ends of the curves correspond to the condition of tangency at Mars, and the low-t_{T0t} end points are for tangency at Earth. Thus, the low-t_{T0t} end points are either perihelion-direct or direct-perihelion paths. This is shown in Fig. 4b, where the $92.9 \cdot 10^6$-r_0 curve from Fig. 3b is included as the boundary of the perihelion-perihelion family.

Figure 4a shows one of a series of envelope curves, which is similar to the one in Fig. 3a, forming the locus of all optimum-$V^2_{0,r}$ points, for specified values of waiting time and $r_{0,d}$. The envelope curves for several values of $r_{0,d}$ are shown in Fig. 4b, and another envelope curve is drawn representing the locus of all optimum-$V^2_{0,r}$ and optimum-$r_{0,d}$ points for zero waiting time. Although complete sets of curves were not drawn for other waiting times, enough points were calculated to indicate that the envelope curves will be in the same relationship to the direct-perihelion curves as illustrated in Fig. 4b.

In the high-t_{T0t} regions, above the possible trip-time range of the direct-perihelion paths, the perihelion-perihelion trajectories offer very little improvement in Δv_{T0t}. At lower trip times, the perihelion-perihelion families are nearly comparable to the best direct-perihelion paths. Note that the $92.9 \cdot 10^6$-mile curve in Fig. 4b is the common boundary of the two families, and that this same curve is very near the optimum envelope in Fig. 3b. However, as will be discussed in connection with the comparison of orbiting paths, differences in required launch

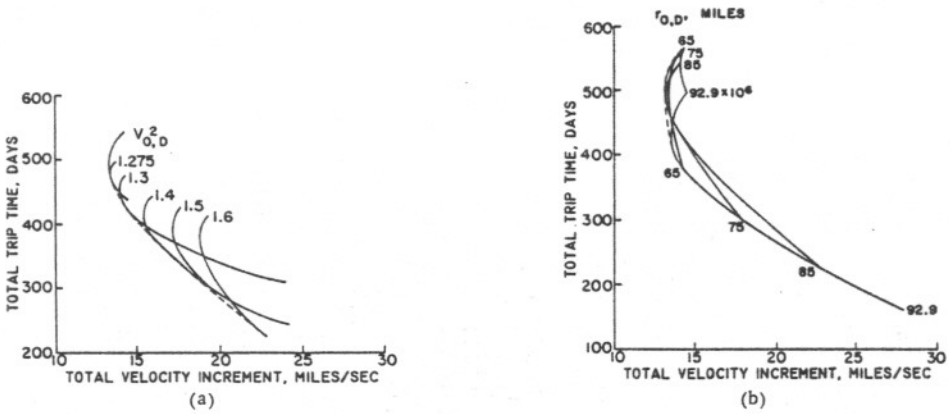

Fig. 4. Characteristics of perihelion-perihelion orbiting round-trip trajectories. a) Total trip time vs total velocity increment. Departure perihelion radius, $r_{0,d}$, $85 \cdot 10^6$ miles; waiting time, t_{wait}, 0 days. b) Total trip time vs total velocity increment. Optimum return path; waiting time, t_{wait}, 0 days.

configuration make perihelion-perihelion paths valuable in providing flexibility of launch date.

The characteristics of "opposition" paths have been included (Fig. 5) to illustrate the price which must be paid to have minimum communication distance at the time the spacecraft is in orbit around Mars. All opposition paths are symmetric perihelion-perihelion round trips. Figure 5a shows the combinations of total time and total velocity increment which result in Earth-Mars opposition at the midpoint of the waiting period. Waiting times up to 60 days are illustrated. The minimum-Δv_{T0t} point for zero waiting time corresponds to a point on the perihelion-perihelion curve (Fig. 4b), while the minimum-t_{T0t} end points correspond to paths tangent to Earth's orbit. Nonsymmetric opposition paths would require higher Δv_{T0t}'s for a specified t_{T0t} than do the symmetric paths.

Figure 5b shows that the low-Δv_{T0t} opposition paths are nearly tangent to Mars' orbit, where $v_{h,M}$ is minimum. The hyperbolic velocity at Earth does not change much with trip time for the lower values of waiting time. Launch constellation is shown in Fig. 5c plotted vs total trip time. Consideration of both Figs. 5a and c reveals that waiting time can be traded for delay in launching. For example, if a spacecraft had a Δv_{T0t} capability of 24 miles per second and could be launched on a certain date for an opposition trip with 60-day waiting time it could also be launched 2 months later and have a waiting period of 10 days.

Swing-Around Paths

CONCEPT. In addition to the general orbiting trajectories, there are special cases which offer interesting advantages at the expense of certain limitations. As described by Battin [2] and Ehricke [1] round trips are possible which require no propulsion at Mars. They are referred to herein as "swing-around" paths. That such paths exist with total trip times of less than two years is not so intuitively obvious. The examples worked out by Battin were restricted to low-energy orbits, and times of 2 to 3 years resulted. Without such a restriction, swing-around paths with total trip times of 1 to 1.5 years can be identified. The

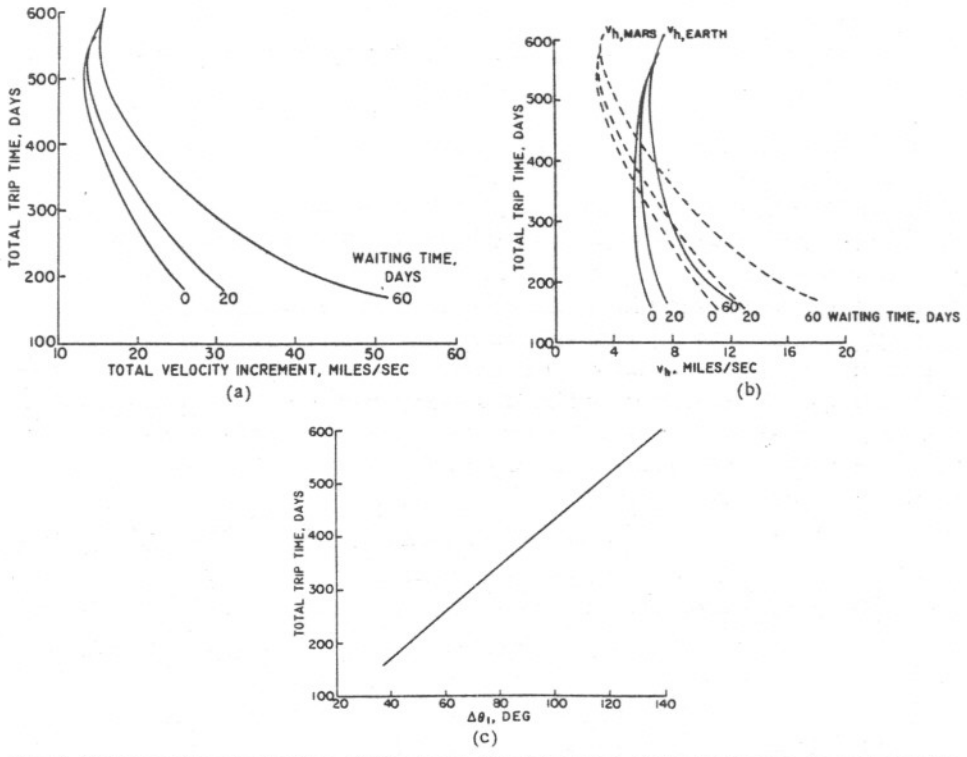

Fig. 5. Characteristics of opposition orbiting round-trip trajectories. a) Total trip time vs total velocity increment. b) Total trip time vs hyperbolic velocities. c) Total trip time vs planetary relative angular position at Earth departure. Mars is ahead of Earth when $\Delta\theta_1 > 0$.

corresponding velocity-increment requirements are not unreasonably high, although certainly higher than those of Battin's examples. In fact, low Δv_{T0t} requirement is the principal advantage of swing-around paths in the comparison with the orbiting round-trip trajectories.

A schematic illustration of some swing-around paths is shown in Fig. 6. The three possible configurations correspond to (1) perihelion, (2) aphelion, and (3) indirect outbound legs. In the perihelion path the spacecraft leaves Earth on a trajectory which takes it nearer to the Sun. After going through perihelion the vehicle crosses the Earth's orbit and reaches Mars at first opportunity. Upon approaching Mars the spacecraft is assumed to follow a hyperbolic path relative to the planet, being deflected by Mars' gravitational field onto a path which will return to the Earth. The spacecraft will be deflected either inward or outward, depending upon which side of the planet the vehicle approaches. In either case, the rocket leaves the vicinity of Mars on a different ellipse, one which will eventually bring it home to Earth. The return leg will be either another perihelion path or an indirect path. The latter is illustrated in Fig. 6a, where the vehicle goes through aphelion, intersects the orbits of both Mars and Earth, and finally makes connections with the Earth at its second crossing of the Earth's orbit.

The other two variations, shown in Figs. 6b and c, differ only in the nature of the outbound path. The aphelion version leaves Earth on an outward trajectory

which reaches Mars at the second crossing of the outer orbit, having passed through aphelion between crossings. The return leg will then be a perihelion path. The indirect outbound path, in Fig. 6c goes through perihelion, aphelion, and both planetary orbits before swinging around Mars and returning by a perihelion path.

Of the other combinations conceivable only one requires comment. If a direct path had been taken to Mars there would be no round trip possible of less than two years duration. The return leg would have to be either an aphelion or an indirect path, but in neither case could the spacecraft meet the Earth on the first time around. It may also be noted that the indirect version illustrated is inferior to the perihelion and aphelion trajectories and will receive no further attention.

A closer look at the hyperbolic encounter is shown in Fig. 7. Since the spacecraft will have a velocity less than that of Mars, the planet will overtake the vehicle. Relative to Mars, the action takes the form illustrated, with the rocket following a hyperbolic trajectory about the planet. At infinity on either end the velocities are the same because no atmospheric braking is assumed. The deflection angle in the Mars coordinates is

$$\psi = \cos^{-1}\left[1 - \frac{2}{(V_{0,m}^2 - 1)^2}\right] \tag{10}$$

where $V_{0,m} = \dfrac{v_0}{v_{c,0}}$ at the vertex of the hyperbola. If the spacecraft passes on the sun side of the planet, it is said to swing out. If the vehicle passes on the outer side, it is said to swing in.

Since the vehicle does not enter a closed orbit about Mars, observation time is limited, but other missions are conceivable for which such a trajectory would be quite suitable. One example is a manned ferry-type mission which would place a payload into orbit about Mars. The principal advantage of the swing-around paths is that a very low total impulse is required compared to other round trips of the same total trip time.

CHARACTERISTICS. Characteristics of the swing-around trajectory families which have perihelion and aphelion outbound paths (Figs. 6a and b) are presented in Figs. 8 and 9, respectively. The five parts of Fig. 8 show total trip time plotted vs (a) total velocity increment, (b) hyperbolic velocity leaving Earth, (c) hyperbolic velocity returning to Earth, (d) planetary relative angular position at

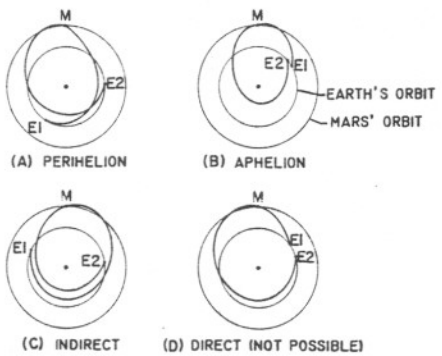

Fig. 6. Schematic of swing-around paths.

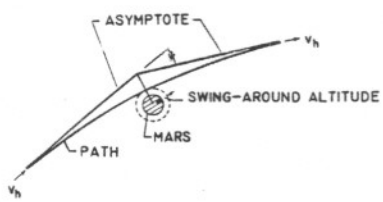

Fig. 7. Schematic of hyperbolic encounter.

Fig. 8. velocit hyperb depart

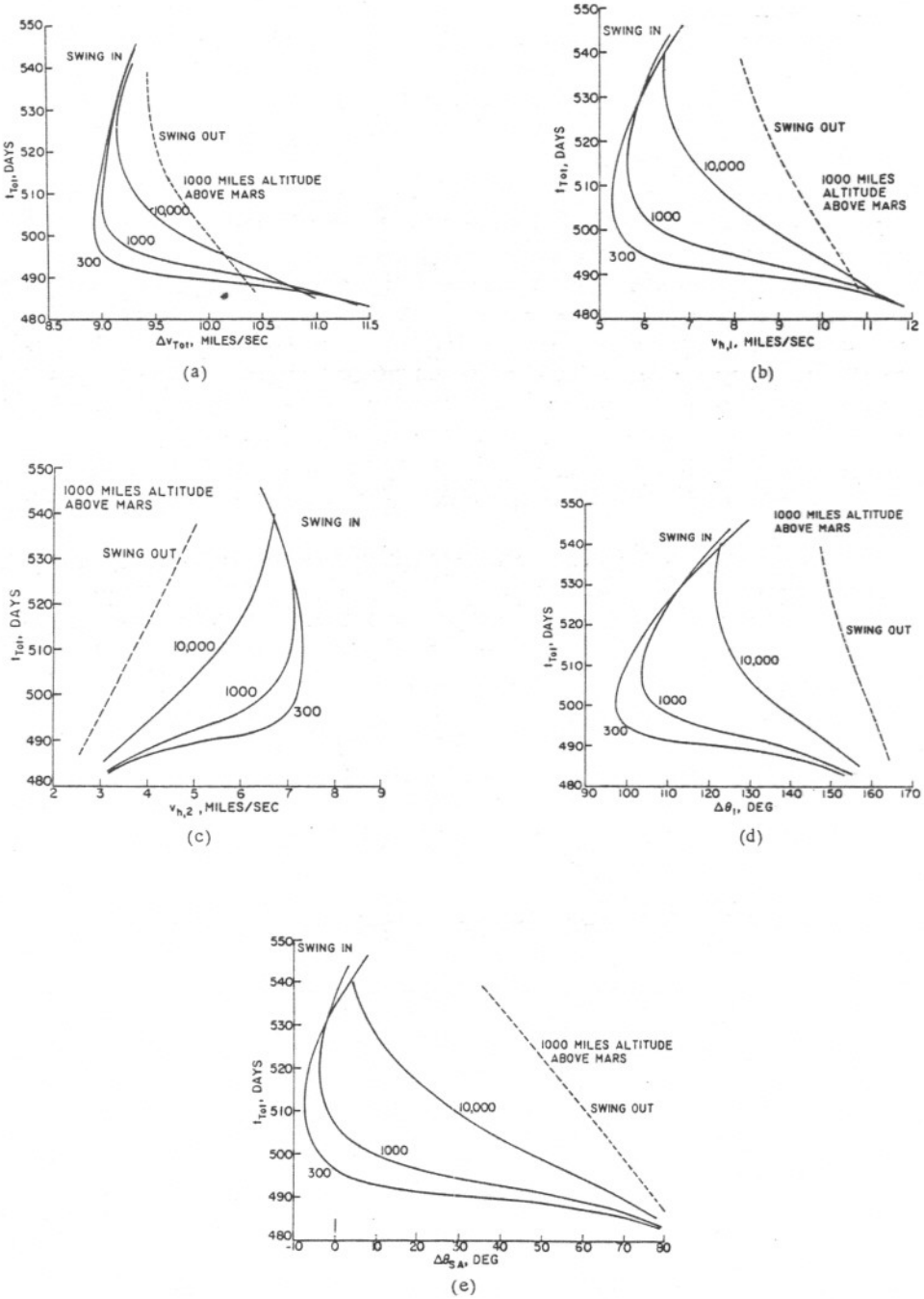

Fig. 8. Characteristics of perihelion swing-around round-trip trajectories. a) Total trip time vs total velocity increment. b) Total trip time vs hyperbolic velocity at Earth departure. c) Total trip time vs hyperbolic velocity at Earth arrival. d) Total trip time vs planetary relative angular position at Earth departure. Mars is ahead of Earth when $\Delta\theta_1 > 0$. e) Total trip time vs planetary relative angular position at swing around. Mars is ahead of Earth when $\Delta\theta_{SA} > 0$.

Earth departure, and (e) planetary relative angular position at swing around. Both swing in and swing out are shown, the former for minimum swing-around altitudes of 300, 1000, and 10,000 statute miles and the latter for 1000 miles.

The end points of the curves in Fig. 8 are very near to the actual limits of the trajectory family. On the high-Δv_{T0t} end the outbound paths are of high energy, and the limit is reached where the deflection due to Mars places the spacecraft on an ellipse which does not intersect the Earth's orbit. At the high-t_{T0t} end the outbound paths are of relatively low energy, and the end points correspond to the condition wherein the transfer ellipses do not reach Mars' radius.

Considering first the swing-in curves of the perihelion family Fig. 8a reveals the presence of minimum values of Δv_{T0t}. Figs. 8b and c indicate that these minima occur while the hyperbolic velocity leaving Earth is reaching a minimum and the returning hyperbolic velocity is reaching a maximum. In each case the increase in $v_{h,2}$ is less pronounced than the reduction in $v_{h,1}$, and the result is a braod minimum in the Δv_{T0t} curve. Note that the time scale covers a space of only 60 days.

The initial angular position of the planets for perihelion swing-around paths is shown in Fig. 8d. Since 60° on the $\Delta\theta_1$ scale corresponds to about a 4-month variation in launch date, the minimum-Δv_{T0t} launch dates fall within a period of about 2 months in each synodic period.

At swing around, the relative angular position of the planets, shown in Fig. 8e, indicates the magnitude of the communication distance. The values of $\Delta\theta_{SA}$ for the minimum-Δv_{T0t} regions fall near zero, the point of closest planetary approach. That such should be the case is not mere coincidence, because minimum-Δv_{T0t} paths correspond to small angles at Mars and the trajectories are nearly symmetrical. Since any symmetrical, zero-wait-time round trip results in either planetary opposition or conjunction, the minimum-Δv_{T0t} swing-around paths could be expected to correspond approximately to Earth-Mars opposition (nearest approach). In fact, a value of $\Delta\theta_{SA}$ up to 43°, taking in most of the swing-around family, represents only a factor of 2 in communication distance.

The curves for the swing-out case do not reveal any great merit for the trajectory in comparison with swing-in paths. The same trip-time range is covered but with greater values of Δv_{T0t} and $\Delta\theta_{SA}$. Furthermore, the initial angular position range is neither large enough nor different enough from that of the swing-in paths to make the variation significant. Thus, beyond recognizing the existence of the swing-out trajectory family no further discussion is warranted.

The characteristics of aphelion swing-around trajectories which "swing-out" at Mars, shown in Fig. 9, present a different picture. In this set of curves the high-Δv_{T0t} ends do not represent limits. Rather, the calculations were discontinued because of the unfavorable Δv_{T0t} magnitude and the fact that the perihelion radius of the return leg had been reduced to 25 million miles. Even at the low-Δv_{T0t} end, where the limit is due to the transfer orbit being tangent to the orbit of Mars, the return path has a perihelion radius of only 41 million miles.

A comparison of Figs. 9a and 8a shows the aphelion swing-around paths to be of shorter duration but higher total velocity increment than are the perihelion paths. The optimum path from a Δv-time standpoint is at the low-Δv_{T0t} end of the curve, but the merit of this trajectory must be judged in comparison with orbiting

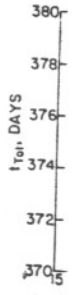

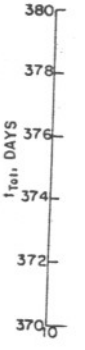

Fig. 9. C
miles. Sw
locity a
vs plan
trip tim

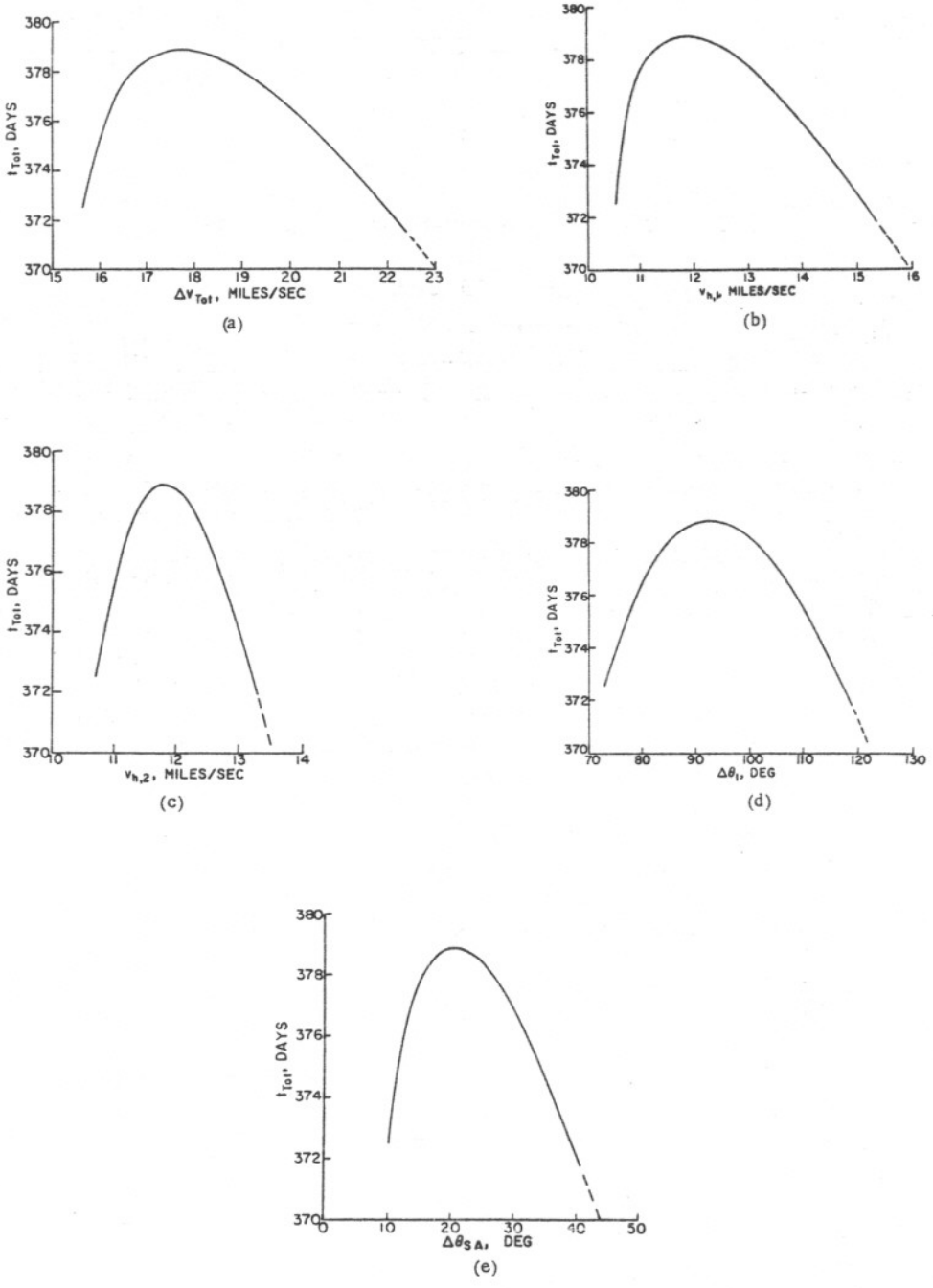

Fig. 9. Characteristics of aphelion swing-around round-trip trajectories. Swing-around altitude, 1000 miles. Swing out. a) Total trip time vs total velocity increment. b) Total trip time vs hyperbolic velocity at Earth departure. c) Total trip time vs hyperbolic velocity at Earth arrival. d) Total trip time vs planetary relative angular position at Earth departure. Mars is ahead of Earth when $\Delta\theta_1 > 0$. e) Total trip time vs planetary relative angular position at swing around. Mars is ahead of Earth when $\Delta\theta_{SA} > 0$.

paths because they occupy the same region on the Δv-time plot. Figures 9b and c show that the hyperbolic velocities at departure and return are very nearly equal at the lower values of Δv_{T0t} and have similar peak values.

Figure 9d indicates that the range of initial planetary constellation is slightly different from that shown in Fig. 8d, with the area of interest covering a launch period of about a month. Figure 9e again shows that the low-Δv_{T0t} swing-around paths correspond to small values of $\Delta\theta_{SA}$. The low-Δv_{T0t} end point, with $\Delta\theta_{SA} = 10°$, represents a communication distance only 8% greater than minimum.

COMPARISON OF TRAJECTORY TYPES

Criteria

The aim of this study of Earth-Mars round-trip trajectories is to apply certain criteria to the multitude of possible path types and indicate which types best satisfy the various requirements. In addition to the total time and total velocity increment criteria used in the partial optimization of the orbiting paths, the other characteristics of interest are (1) choice of launch date and waiting time, (2) short communication distance, and (3) insensitivity to departure velocity vector error. The comparison procedure is to make the preliminary selection of areas of interest by means of $t_{T0t} - \Delta v_{T0t}$ plots and then indicate the expected behavior of these trajectories with respect to the other criteria.

Orbiting Paths

Moeckel [3] has published the characteristics of orbiting round trips which are made up of paths tangent to one of the planetary orbits. Symmetric round-trip trajectories, which have departure and return paths along ellipses of the same shape, are shown to exhibit discontinuities in required waiting time at Mars. The points where waiting time goes to zero are called "breakthroughs". Except near the breakthroughs the tangent families require high waiting times (up to 780 days). Three of the lowest-t_{T0t} breakthroughs are indicated in Fig. 10.

Since long waiting times do not appear to be necessary for Mars observation and would probably be disadvantageous from several standpoints, interest is drawn to the low-waiting-time trajectories. Moeckel [3] also combined tangent paths into nonsymmetric round trips, the only requirements being that the departure path be tangent to Earth's orbit and the return leg be tangent to Mars' orbit. The resulting family of zero-waiting-time trajectories is plotted in Fig. 10, showing a considerable improvement over the symmetrical breakthrough points.

In Fig. 10 are also plotted the envelope curves from Figs. 3c and 4b. The upper end of the perihelion-perihelion curve is shown to be the breakthrough point of the corresponding tangent-at-Mars family, and the lower end of the direct-perihelion curve is the breakthrough point of the direct-direct tangent-at-Earth family. The fact that the tangent and nontangent direct-perihelion curves are not tangent may be due to Moeckel's [3] calculations having been based on orbits with radii equal to 1.1 times the planets' radii.

The smallness of the Δv_{T0t} difference between the perihelion-perihelion and direct-perihelion paths is shown clearly in Fig. 10. A total velocity increment of about 13 miles per second appears to be the lower limit for orbiting round trips, and the corresponding time range is from 450 to 500 days. As the trip time is

further reduced Δv_{T0t} increases at an accelerating rate. As a result, a one-year trip requires a Δv_{T0t} of 14.4 miles per second, while a 0.5-year flight requires 26.2 miles per second.

The nontangent trajectories are shown to have some superiority over the tangent paths. Actually, the optimum direct-perihelion trajectories leave Earth tangent or nearly tangent to the planet's orbit. The return flight is generally tangent to neither orbit, and the reduction in Δv_{T0t} shown in Fig. 10 results. Similar trajectories have been reported by Ehricke [1], showing low-waiting-time direct-perihelion paths of less than a year duration. The principal extension of the present results over those of [1] is that the entire family of trajectories for each specified waiting time is presented rather than one point for each t_{wait}.

Curves for higher waiting times and for opposition paths will be added in conjunction with later sections, wherein choice of waiting time and communication distance are discussed. It is sufficient at this point in the comparison to note that the curves fall to the right of the zero-waiting-time curves.

Swing-Around Paths

On a plot of total trip time vs total velocity increment, such as Fig. 11, swing-around trajectories appear in several widely separated areas. Fig. 11 shows the paths of Figs. 8a and 9a and, also, one of the longer-duration nonstop trajectories calculated by Battin [2]. The Δv_{T0t} for the latter point was calculated using the eccentricity and semimajor axis quoted in [2] for a round-trip path leaving tangent to Earth's orbit on a 164-day outbound leg and returning on an indirect path, going 1.5 revolutions around the sun before making connections with the Earth. Although the Δv_{T0t} shown is less than that of the Hohmann minimum-energy path, the fact that the time is greater probably destroys any hope of acceptance in practice.

The aphelion swing-around path can also be virtually eliminated from further consideration on the basis of its inferior showing in relation to the best orbiting paths. It seems improbable that the simplicity of having no propulsion period at Mars will outweigh the indicated difference in Δv_{T0t} requirement, at least for relatively high-thrust vehicles. However, there is a possible exception to this

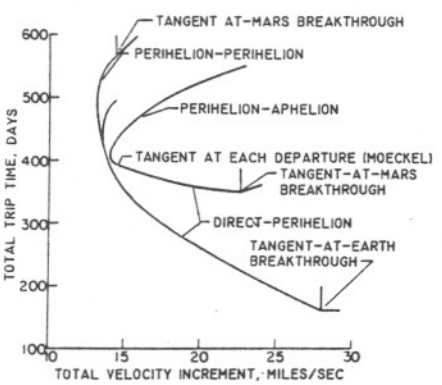

Fig. 10. Comparison of orbiting round-trip trajectories. Waiting time, t_{wait}, 0 days.

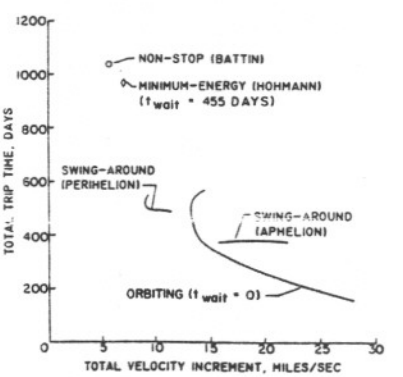

Fig. 11. Comparison of orbiting and swing-around round-trip trajectories.

argument, which may actually make the trajectory very attractive. A very-low-thrust vehicle, such as one using ion propulsion, is limited in its low-waiting-time capability by the time required to decelerate and accelerate at Mars. On a swing-around path such an extended propulsion period is not needed, and most missions could be accomplished by causing any Mars-destined payload to be put into orbit with its own propulsion system. However, consideration of this application must be taken up in comparison with continuous-thrust trajectories and is beyond the scope of this paper.

The perihelion swing-around paths are shown to offer a considerable advantage in Δv_{T0t} over the lowest-energy orbiting paths. The trip time range of 485 to 540 days is about 100 days greater than the region of lowest-Δv_{T0t} direct-perihelion orbiting paths, and the narrowness of the span does not allow improvement with vehicle capability. Thus the swing-around family is very much a special case. Final evaluation of its merits will necessarily come from economic and functional considerations, but the importance of the indicated reduction in Δv_{T0t} should be carefully considered.

Other Considerations

CHOICE OF WAITING TIME. One form of flexibility which the orbiting paths possess is variable waiting time at Mars. The envelope curves of Fig. 3c for direct-perihelion orbiting paths with 0, 30, and 60 days waiting time are combined with corresponding curves for perihelion-perihelion paths in Fig. 12, only the envelope of the two families being plotted. Thus, there is a minimum Δv_{T0t} required for an orbiting round trip of a specified waiting time. Above the minimum velocity increment it is possible to accept a higher total trip time in return for a longer waiting period at Mars.

Another form of flexibility allows a choice of waiting time after arrival at Mars by deviation from the family of optimum trajectories. Figure 13 illustrates the choice of return flight available over a range of planetary relative angular position. For example, if a 150-day return flight is scheduled for the date on

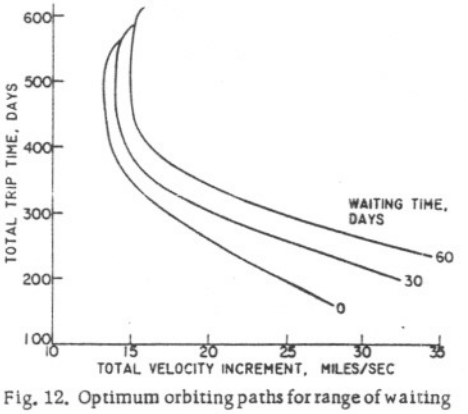

Fig. 12. Optimum orbiting paths for range of waiting time.

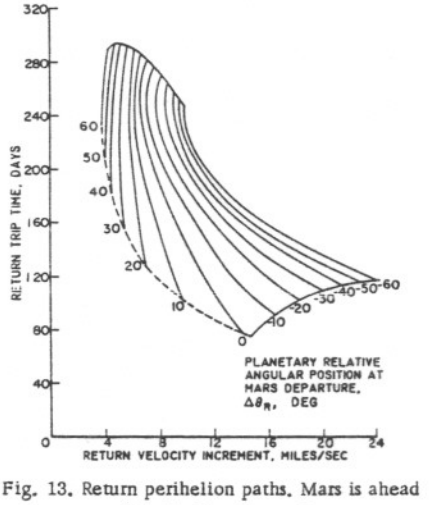

Fig. 13. Return perihelion paths. Mars is ahead of Earth when $\Delta\theta_R > 0$.

which Mars is 10° ahead of the Earth ($\Delta\theta_R = 10°$), it would be possible to extend the waiting period at Mars by a month with no change in required Δv_{T0t} by taking a return path of 200-day duration ($\Delta\theta_R = -5°$). Such a choice exists when Mars is less than 20° ahead of the Earth, and the penalty in return trip time for a lengthening of the waiting period diminishes as the available return Δv increases.

CHOICE OF LAUNCH DATE. The sensitivity of trajectory characteristics to launch date is shown in the figures which specify values of $\Delta\theta_1$ for the several trajectory families. Fig. 8d, for perihelion-swing-around paths, covers a range of launch date of about 4 months. However, the total velocity increment varies over this range also, and the most interesting observation is the range of launch date for a specified Δv_{T0t}. A comparison of Figs. 8a and d reveals that the altitude range from 300 to 10,000 miles above Mars' surface corresponds to a 30-day launch date span at Δv_{T0t} = 9.5 miles per second. The range of launch date is relatively uniform over the Δv_{T0t} interval, increasing to a maximum of about 40 days at the minimum Δv_{T0t} for 10,000-mile-altitude paths. Thus, if the navigational system were accurate enough, a delay in launch date could be obtained by reducing the swing-around altitude. Unfortunately, the most desirous conditions, low-Δv_{T0t} and low altitude, correspond to the latest date.

To assess the launch-date flexibility of orbiting paths the direct-perihelion and perihelion-perihelion families should be considered together. As shown in Figs. 3b and 4b, the envelopes of the two families lie very close on a Δv-time plot. In the area on the upper-right-hand side of the $92.9 \cdot 10^6$-mile curve, which is the common member of the two families, a specified trip time can be obtained for a specified value of total velocity increment with either type of round-trip trajectory. However, the launch constellations for the two types are quite different.

Figure 3e shows that the values of $\Delta\theta_1$ for direct-perihelion paths are on the low side of about 40°. The corresponding values for perihelion-perihelion paths lie above 40°, as is indicated in Fig. 5c. A launching period can be imagined which would (1) begin on the earliest date when a perihelion-perihelion path of a specified maximum duration is possible for a specified Δv_{T0t}, (2) proceed with shorter flights or higher payloads through the perihelion-perihelion family into the direct-perihelion family, (3) reach the date on which the shortest flight or the largest payload is possible (when $\Delta\theta_1$ is in the range of 20° to 40°), (4) proceed with longer flights or lower payloads through the direct-perihelion family, and (5) end on the date when a Δv_{T0t} higher than the vehicle's capability is required to obtain the specified low waiting time. For example, if the Δv_{T0t} capability were 16 miles per second and total trip times less than 485 days were acceptable the total launching period would extend over a span of about 8.5-months. If trip time is allowed to decrease as optimum conditions are approached, a minimum t_{T0t} of 327 days will be reached about one month from the end of the launch period.

COMMUNICATION DISTANCE. One of the common characteristics of short-waiting-time round-trip trajectories is that of low communication distance during the time the spacecraft spends at Mars. Figures 3f, 8e, 9e, and the appendix work charts reveal this generality. The only cases wherein $\Delta\theta_W$ or $\Delta\theta_{SA}$ exceed the value for a communication distance twice minimum are at extremes of the trajectory families which are furthest from optimum.

An indication of the relationship between the true opposition and the optimum orbiting trajectories is given in Fig. 14. Two waiting times, zero and 60 days, are illustrated. For large spacecraft, the increase in payload capability reflected by the Δv_{T0t} decrement would probably more than offset the weight of communication equipment needed to transmit over the increased distance.

MISS COEFFICIENTS. Magness, McGuire, and Smith [5] discuss the theoretical possibility of "guidance minima", which are combinations of trajectory parameters for which sensitivity to Earth-departure velocity or angle approach zero. For example, if the partial derivative, $\partial b/\partial\lambda$, where b is the miss distance at Mars and λ is a function of burnout velocity, should be zero, we can say that, to the first order, the miss distance at Mars will not change with errors in burnout velocity. Similarly, miss distance will be insensitive to burnout angle when $\partial b/\partial\beta$ goes to zero. The two derivatives, or "miss coefficients", are shown to have no common vanishing conditions, but certain regions exist wherein both are low.

Reference [5] contains curves of velocity and angle miss coefficients for flights from Earth to Mars with Earth-departure velocities less than 22.7 miles per second and angles to Earth's orbit up to ±14°. These ranges restrict, somewhat, the evaluation of the high-energy trajectories which are the subject of this study. However, Fig. 15 has been prepared to indicate the extent to which the perihelion swing-around paths and the optimum orbiting paths can be expected to show insensitivity to burnout-velocity-vector error. The direct-perihelion paths for perihelion radii of 92.9 and $85 \cdot 10^6$ miles are used to define the region in which the optimum paths lie. The swing-around curve is for an altitude of 1000 miles above Mars' surface.

With respect to the velocity miss coefficient alone the situation looks good for either family, as shown in Fig. 15a. The swing-around path which has the highest trip time is approximately a velocity guidance minimum. This is also true for other swing-around altitudes. For the orbiting trajectories, the values of velocity miss coefficient are relatively small over the range of trip times below 470 days. In particular, the region around 300 days, wherein a perihelion radius of $85 \cdot 10^6$ miles is optimum, exhibits the interesting characteristic of an extended guidance

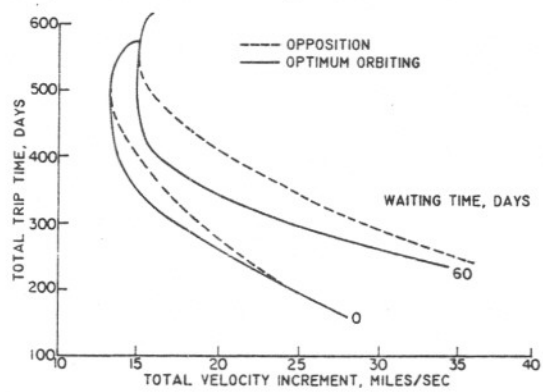

Fig. 14. Comparison of optimum orbiting and opposition round-trip trajectories.

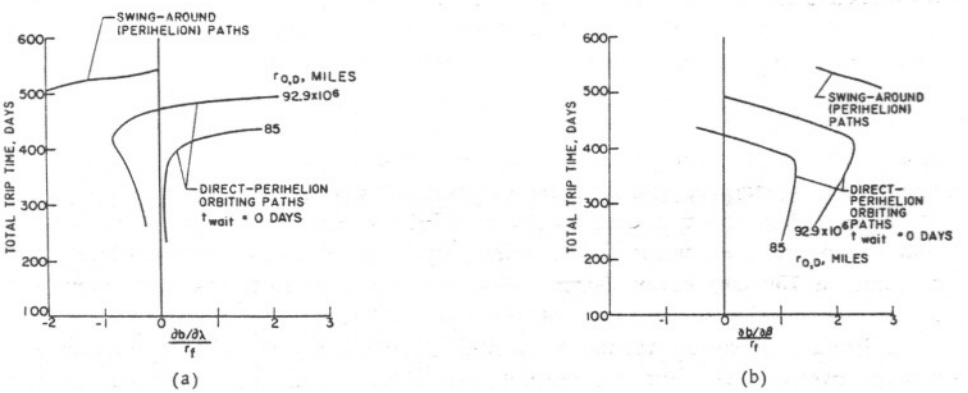

Fig. 15. Miss coefficients for departure paths. a) Total trip time vs velocity miss coefficient. Velocity parameter, $\lambda \equiv (v_1/18.5)^2$; radius of Mars' orbit, r_f, $141.5 \cdot 10^6$ miles. b) Total trip time vs angle miss coefficient. Departure angle, $\beta \equiv 90° - \alpha_1$; radius of Mars' orbit, r_f, $141.5 \cdot 10^6$ miles.

minimum. Practical exploitation of guidance minima would seem to depend upon such an occurrence if flexibility of trip time or launch date is to be realized. The relatively small change in velocity miss coefficient with swing-around altitude is also compatible with flexibility of launch date.

The values of angle miss coefficient, shown in Fig. 15b, are not as accommodating. Although no evidence is available to indicate the penalties associated with particular magnitudes of miss coefficients, the swing-around paths are shown to exhibit minimum angle miss coefficients considerably higher than the best velocity coefficients of Fig. 15a. Because of the approximate nature of the magnitudes plotted, it is more pertinent to observe from [5] that no guidance minima exist in the range of velocities typical of swing-around paths, the theoretical minimum value being about 0.75. Likewise, the orbiting paths, although exhibiting guidance minima at high trip times, are indicated to have relatively high miss coefficients over the useful trip-time range.

Miss coefficients for return trajectories were not included in [5]. Extension to such cases was not considered warranted because of the uncertainties with regard to the application of this type of analysis and the importance of three-dimensional effects.

CONCLUSIONS

1. Of the many possible Earth-Mars round-trip trajectories, two families have particular merit: (a) low-waiting-time orbiting paths, and (b) perihelion swing-around paths.

2. Orbiting paths offer flexibility of trip time and waiting time. Minimum values of total velocity increment of representative zero-waiting-time trajectories are as follows:

t_{Tot}, days	Δv_{Tot}, miles/second
450	13.3
365	14.4
182	26.2

An increase in waiting time at Mars can be obtained by an increase in either $\Delta v_{T0\ell}$ or . At a specified value of total velocity increment, an increase in waiting time results in a slightly lengthened coasting period, the two time increments contributing to an increased total trip time.

3. Orbiting paths also offer flexibility of launch date and return flight if deviation from optimum conditions is allowed. At a $\Delta v_{T0\ell}$ capability of 16 miles per second, an 8.5-month launch period can be obtained by accepting a 485-day total trip time. Minimum trip time would be 327 days. After arrival at Mars, waiting time can be extended without $\Delta v_{T0\ell}$ change by accepting longer return flights. For example, a 150-day return flight on a date when Mars is 10° ahead of Earth can be replaced by a 30-day waiting period and a 200-day return flight.

4. Perihelion swing-around paths offer a considerable velocity-increment advantage over the best orbiting trajectories. However, only a narrow span of trip times is possible, and no waiting time at destination is permitted. The least-energy path in this family has a total trip time of 508 days and a total velocity increment of 9 miles per second.

5. Launch date for perihelion swing-around paths can be varied by altering the altitude of closest approach to Mars. At a total-velocity-increment capability of 9.5 miles per second, a 30-day delay in launch date corresponds to an altitude reduction from 10,000 to 300 statute miles.

6. On a total trip time and total velocity-increment basis, aphelion swing-around paths are inferior to optimum orbiting trajectories. However, one possible application of the swing-around path would be for low-thrust systems which could not enter a circular orbit without an excessively long propulsion period.

7. Communication distances when the spacecraft is at Mars are relatively short for all near-optimum round-trip trajectories of the swing-around or short-waiting-time orbiting families. The communication distance exceeds twice minimum only for extremes of the trajectory families which are furthest from optimum.

8. Sensitivity to Earth-departure velocity vector error appears to be about equal for the two trajectory families. With respect to velocity magnitude, extended guidance minima are found near the optimum-$\Delta v_{T0\ell}$ regions. Corresponding angle miss coefficients have higher values, but associated penalties are not known.

9. The simplifying assumptions upon which the study is based make the resulting comparison of round-trip trajectories preliminary in nature. Three-dimensional calculations which optimize the transition from one orbital plane to another and which account for the eccentricity of the planetary orbits are required to complete the picture. The two-dimensional, circular-orbit analysis is intended to serve as a guide in the more exact investigations, to the ultimate reduction of work. Also, for the initial direction of preliminary design studies and systems analyses, the simplified study has been found useful and may assist in promoting consistency of ground rules for other aspects of space research and development.

APPENDIX

WORK CHARTS AND ROUND-TRIP COMPUTATION PROCEDURE. Solutions to the basic equations presented in the Methods section have been obtained for ranges of r_0 and V_0^2 and plotted in a set of work charts (Figs. 16 to 20). At each r_0, V_0^2 varies from the lower limit, which produces a path tangent to Mars' orbit, to an arbitrary upper limit of 1.9. The perihelion radius is allowed to vary from an arbitrary lower limit of 55 million miles to the radius of the Earth's orbit.

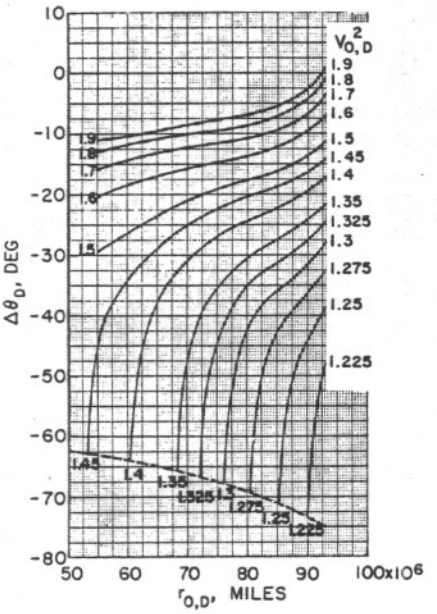

Fig. 16. Earth-Mars direct path: planetary relative angular position at Mars arrival vs perihelion radius of path. Mars is ahead of Earth when $\Delta\theta_D > 0$.

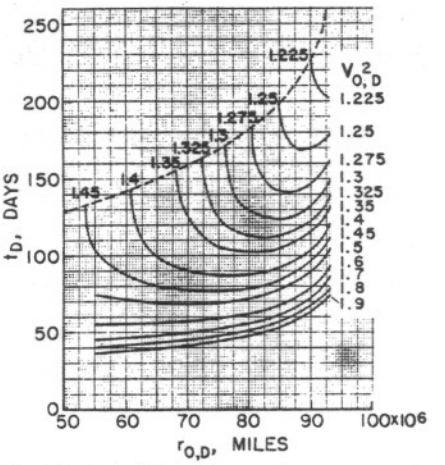

Fig. 17. Earth-Mars direct path: one-way trip time vs perihelion radius of path.

The lower limit of r_0 has proven in use to be somewhat restrictive. Very-low-energy orbiting trajectories, which define the high-t_{T0t} end of the curves in Fig. 3, were estimated from extrapolations of the limit lines of Figs. 18 to 20.

The work charts are based on the basic data given in Table I, and the values of Δv given in Fig. 18 are for Earth and Mars satellite orbits of 300- and 1000-statute mile altitude, respectively.

The procedure used in constructing a round trip from a direct departure path and a perihelion return path is as follows:

1. Specify $r_{0,d}$ and $V^2_{0,d}$
2. Entering Fig. 16 with $r_{0,d}$ and $V^2_{0,d}$, read $\Delta\theta_D$
   Note: $\Delta\theta_D$ is the planetary relative angular position at the end of the departure path
3. Read t_D from Fig. 17
4. Read Δv_D from Fig. 18
5. Specify $V^2_{0,r}$

6. Compute $\Delta\theta_R = \Delta\theta_D - 0.461\, t_{wait}$, where 0.461 is the rate of change of Earth-Mars constellation in degrees per day and t_{wait} is the waiting time in days
7. Entering Fig. 19 with $\Delta\theta_R$ and $V^2_{0,r}$, read $r_{0,r}$
8. Entering Fig. 18 with $r_{0,r}$ and $V^2_{0,r}$, read Δv_R
9. Similarly, read t_R from Fig. 20
10. Calculate $\Delta v_{Tot} = \Delta v_D + \Delta v_R$
11. Calculate $t_{Tot} = t_D + t_R + t_{wait}$

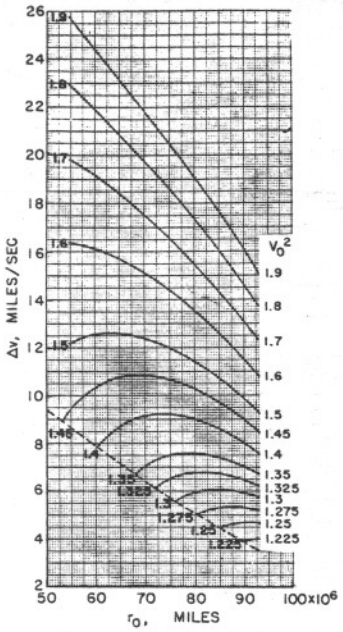

Fig. 18. Sum of Earth and Mars velocity increments for one-way trip vs perihelion radius of path.

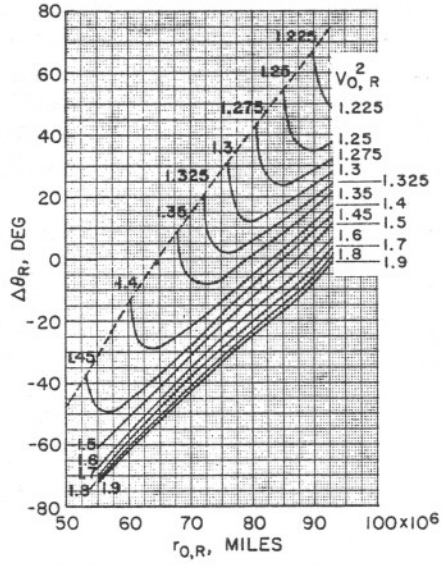

Fig. 19. Mars-Earth perihelion path: planetary relative angular position at Mars departure vs perihelion radius of path. Mars is ahead of Earth when $\Delta\theta_R > 0$.

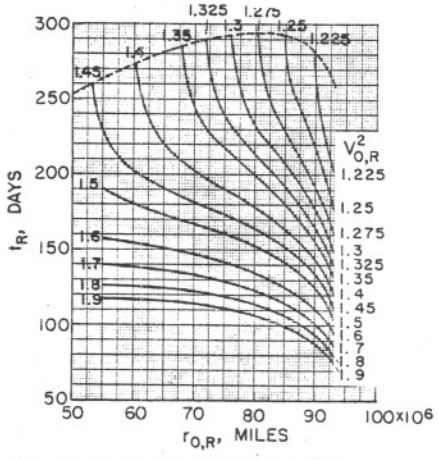

Fig. 20. Mars-Earth perihelion path: one-way trip time vs perihelion radius of path.

The procedure used to construct a round trip from two perihelion paths is modified to the following extent:

1. Specify $r_{0,d}$ and $V^2_{0,d}$

2. Entering Fig. 19 with $r_{0,d}$ and $V^2_{0,d}$, read a value of $\Delta\theta$, reverse its sign, and call it $\Delta\theta_D$. (Fig. 10 is drawn up for a return path and the values of $\Delta\theta$ must be reversed in sign if used for a departure path)

3. Entering Fig. 20 with $r_{0,d}$ and $V^2_{0,d}$, read t_D. Proceed with steps (4) through (11) as above.

REFERENCES

1. K. A. Ehricke, et al, Calculations on a Manned Nuclear Propellant Space Vehicle, ARS Report 532-57, December 1957
2. R. H. Battin, The Determination of Round-Trip Planetary Reconnaissance Trajectories, IAS Report No. 59-31, January 1959
3. W. E. Moeckel, Interplanetary Trajectories with Excess Energy. Presented at the 9th Annual Congress of the International Astronautical Federation, Amsterdam, Netherlands, August 25 to 30, 1958
4. M. Vertregt, Interplanetary Orbits. Journal of the British Interplanetary Society, Vol. 16, No. 6, pp. 326-354, March-April 1958
5. T. A. Magness, et al., Accuracy Requirements for Interplanetary Ballistic Trajectories. Presented at 9th Annual Congress of the International Astronautical Federation, Amsterdam, Netherlands, August 25 to 30, 1958

ıge of Earth-
time in days

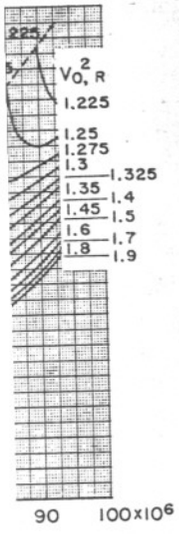

path: planetary
ars departure vs
is ahead of Earth

AN AMERICAN ASTRONAUTICAL SOCIETY PUBLICATION

American Astronautical Society.
... Proceedings [of the] meeting.

ADVANCES in the ASTRONAUTICAL SCIENCES

Volume 5

Proceedings of the
Second Western National Meeting
of the
American Astronautical Society
Los Angeles, California
August 4 - 5, 1959

distributed by:
PLENUM PRESS, INC., NEW YORK

1960